Time-Dependent Modeling of Brillouin Scattering in Optical Fibers Excited by a Chirped Diode Laser

Carl E. Mungan, Steven D. Rogers, Naresh Satyan, *Member, IEEE*, and Jeffrey O. White, *Member, IEEE*

***Abstract*— Numerical simulations are used to solve the coupled partial differential equations describing stimulated Brillouin scattering (SBS) built up from random thermal phonons as a function of time and the longitudinal spatial coordinate in an optical fiber. In the case of a passive fiber, a laser beam is incident with constant power, but its frequency is linearly ramped at 1.55 μm at a rate of up to 10^{16} Hz/s. High chirp rates lead to an increased Brillouin spectral bandwidth and decreased gain. The resulting SBS suppression is well described by an adiabatic model and agrees with experimental results. For an 18-m active fiber pumped at 1.06 μm and chirped at up to 2×10^{16} Hz/s, the suppression enables output laser powers in the kilowatt range while maintaining a narrow instantaneous linewidth.**

***Index Terms*— Brillouin scattering, chirped lasers, fiber amplifiers, numerical simulation**

I. Introduction

BRILLOUIN scattering is one of the lowest order nonlinear effects that arises in optical fibers and it thus limits the transmitted laser power P_L. Above a threshold incident laser power P_{th}, the Brillouin scattering becomes stimulated rather than spontaneous and the Stokes backscattered power P_S rises dramatically. Various methods have been proposed to increase the threshold [1]–[5]. In the present paper, we analyze the effect of linearly sweeping the frequency of the pump laser at a fast chirp rate β. To be effective, the chirp must be large enough that the pump laser is swept out of the Brillouin gain bandwidth $\Delta\nu_B$ within the transit time of the fiber, $t_f = nL/c$, where L is the length of the fiber, n is the core refractive index, and c is the speed of light. That is, one requires β to be large enough that $t_f >> t_c$ where $t_c = \Delta\nu_B/2\beta$. (The factor of 2 comes from the fact that the laser and Stokes waves are counterpropagating in the fiber.) Here we analyze values of β up to 2×10^{16} Hz/s, close to the upper range of chirping that has been demonstrated to date for a diode laser by ramping its current [6], [7].

Section II describes numerical simulations of the Brillouin scattering in a passive fiber with an incident laser beam that is chirped. Section III then presents the simulation results for a 6-km fiber. Such long fibers have a low threshold because $P_{th} \approx 21A/g_0L$ in the unchirped case, where A is the modal area and g_0 is the peak Brillouin gain coefficient. Consequently, low laser powers can be used to experimentally verify the simulations. Agreement is found between theory and measurements. Next, Sec IV presents results of the time-dependent simulations for a short fiber ($L = 17.5$ m) having characteristics similar to those used for high-power laser delivery. Correspondingly larger chirps are needed to suppress stimulated Brillouin scattering (SBS) in this case. The results agree with an adiabatic model that depends on frequency (instead of time) for chirps ranging up to 10^{16} Hz/s. Finally, Sec V adds laser gain to the simulations to predict the output power from a fiber amplifier. Chirping the input laser beam at 2×10^{16} Hz/s enables one to reach the kilowatt range by increasing the SBS threshold.

II. Theory for the Dynamic Simulations

The Brillouin scattering is modeled by three complex coupled partial differential equations (PDEs) [8],

$$\frac{\partial E_L}{\partial z} + \frac{n}{c}\frac{\partial E_L}{\partial t} = \frac{\zeta - \alpha}{2}E_L + i\kappa E_S\rho, \tag{1a}$$

$$-\frac{\partial E_S}{\partial z} + \frac{n}{c}\frac{\partial E_S}{\partial t} = \frac{\zeta - \alpha}{2}E_S + i\kappa E_L\rho^*, \quad \text{and} \tag{1b}$$

$$\frac{\partial \rho}{\partial t} + \pi\,\Delta\nu_B\rho = i\Lambda E_L E_S^* + f. \tag{1c}$$

We checked that adding the two extra derivative terms from (8) in [5] to the left-hand side of (1c) did not noticeably change our simulation results; so for computational simplicity, those terms are omitted. Here the laser electric field $E_L(z,t)$, Brillouin Stokes-shifted field $E_S(z,t)$, and density variation $\rho(z,t)$ of the fiber from its mean value ρ_0 depend on time t and longitudinal position z, varying from $z = 0$ at the front face of the fiber to $z = L$ at the rear face. The spectral full-width-at-half-maximum (FWHM) of the spontaneous Brillouin peak is $\Delta\nu_B$. For a silica fiber at an incident laser wavelength of $\lambda_L = 1.55$ μm, the refractive index is $n = 1.447$, the mean density is $\rho_0 = 2210$ kg/m^3, and the speed of sound

Manuscript received June 29, 2012; revised October 8, 2012; accepted October 14, 2012. Date of publication October 18, 2012; date of current version October 31, 2012. This work was supported in part by the High Energy Laser Joint Technology Office under Grant 11-SA-0405.

C. E. Mungan is with the Physics Department, U.S. Naval Academy, Annapolis, MD 21402 USA (e-mail: mungan@usna.edu).

S. D. Rogers was with the U.S. Army Research Laboratory, Adelphi, MD 20783 USA (e-mail: rogers1@umbc.edu).

N. Satyan is with the Department of Applied Physics and Materials Science, California Institute of Technology, Pasadena, CA 91125 USA (e-mail: naresh@caltech.edu).

J. O. White is with the U.S. Army Research Laboratory, Adelphi, MD 20783 USA (e-mail: jeffrey.owen.white@us.arl.mil).

Color versions of one or more of the figures in this paper are available online at http://ieeexplore.ieee.org.

Digital Object Identifier 10.1109/JQE.2012.2225414

0018–9197/$31.00 © 2012 IEEE

is $\upsilon = 5960$ m/s [8]. The loss coefficient in the fiber is $\alpha = 0.2$ dB/km $= 0.0461$ /km. The laser gain ζ is taken to be independent of t and z for simplicity; $\zeta = 0$ for a passive fiber. The optic coupling parameter is [8]

$$\kappa = \frac{\pi\,\gamma}{2n\rho_0\lambda_{\mathrm{L}}M} \tag{2}$$

where the electrostriction coefficient is $\gamma = 0.902$ [9] and the polarization is presumed to be completely scrambled in the fiber so that $M = 1.5$ [10]. The acoustic coupling parameter is [8]

$$\Lambda = \frac{\pi n\varepsilon_0\gamma}{\lambda_{\mathrm{L}}\upsilon} \tag{3}$$

where ε_0 is the permittivity of free space. The Langevin noise source $f(z,t)$ is delta-correlated in time and space such that [11]

$$\left\langle f(z,t)f*(z',t')\right\rangle = Q\,\delta(z-z')\delta(t-t') \tag{4}$$

where the thermal phonons are described by the strength parameter

$$Q = \frac{4\pi kT\rho_0\Delta\nu_{\mathrm{B}}}{\upsilon^2 A}. \tag{5}$$

Here k is Boltzmann's constant, $T = 293$ K is room temperature, and A is the fiber modal area.

The three PDEs (1) are solved by iterated finite-difference approximations on a grid of time and space points [12]. The spatial step size dz is chosen to be small enough that a factor of two reduction does not change the final values in (8) below by more than 10%. The temporal step size is $dt = n\,dz/c$. The boundary conditions are $E_{\mathrm{S}}(L,t) = 0$ and

$$E_{\mathrm{L}}(0,t) = \sqrt{\frac{2P_0}{nc\varepsilon_0 A}}\exp\left[i\pi\beta\,(t+nL/c)^2\right] \tag{6}$$

where P_0 is the constant laser power incident at $z = 0$. The argument of the exponential is the chirped phase

$$\varphi(t,z) = 2\pi\int_0^{t+n(L-z)/c}\beta t'dt' \tag{7}$$

evaluated at $z = 0$. The three complex fields are first calculated along the fiber for times up to $t = 20t_{\mathrm{f}}$ to ensure that the initial relaxation oscillations [13] have decayed away. The equations are then iterated over 5 more transit times to acquire a statistical average. The transmitted laser power P_{L} and reflected Stokes power P_{S} are computed by averaging over those additional steps

$$\begin{aligned} P_{\mathrm{L}} &= \tfrac{1}{2}nc\varepsilon_0 A\left\langle|E_{\mathrm{L}}(L,t)|^2\right\rangle \quad \text{and} \\ P_{\mathrm{S}} &= \tfrac{1}{2}nc\varepsilon_0 A\left\langle|E_{\mathrm{S}}(0,t)|^2\right\rangle. \end{aligned} \tag{8}$$

The results were checked by verifying that $P_{\mathrm{L}} \approx (P_0 - P_{\mathrm{S}})\exp(-\alpha L)$ in a passive fiber, and agreement was found to within about 1% at zero chirp.

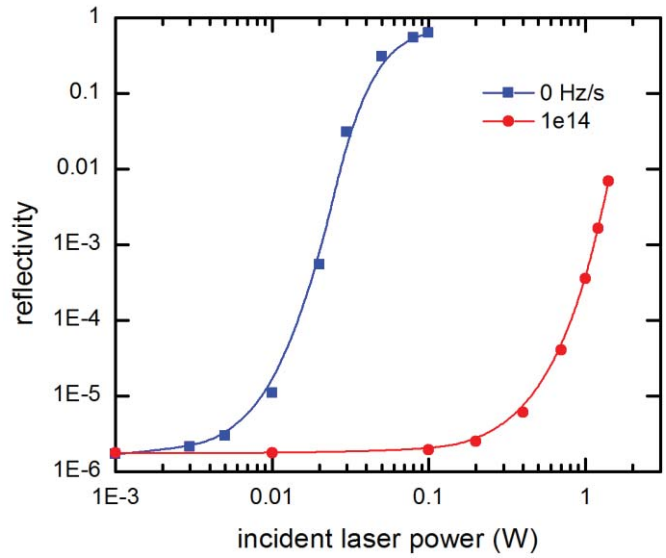

Fig. 1. Brillouin reflectivity versus power for both an unchirped ($\beta = 0$) and a chirped (at $\beta = 10^{14}$ Hz/s) laser beam incident on a long fiber.

III. Dynamic Results for a Long Passive Fiber Compared to Experiment

We calculated P_{S} as a function of P_0 for a passive 6-km single-mode fiber. The FWHM of the spontaneous Brillouin peak was measured to be $\Delta\nu_{\mathrm{B}} = 39$ MHz using a heterodyne technique with an RF spectrum analyzer [7]. The fiber modal area was measured to be $A = \pi r^2$ with $r = 4.55$ μm by a knife-edge scan in the far field.

The reflectivity P_{S}/P_0 is plotted in Fig. 1 for both an unchirped and a chirped laser. For incident powers well below threshold, the reflectivity levels off to a spontaneous value that is independent of chirp and is in good agreement with the experimental value of $R_0 = (3.0 \pm 0.5) \times 10^{-6}$ measured using an optical spectrum analyzer (OSA). On the other hand, for large incident powers the reflectivity approaches 100%. The threshold (defined as the incident power at which the reflectivity is equal to 1%) is approximately two orders of magnitude larger in the chirped case than in the unchirped case.

To directly compare these results to the experimental data, the total backscattered power is next plotted in Fig. 2 as a function of P_0. This backscattered power is the sum of the Rayleigh power $P_{\mathrm{R}} = 2.3 \times 10^{-4}P_0$ determined from low-power OSA measurements and the Brillouin Stokes power P_{S} from Fig. 1. The agreement is reasonable between experiment and theory with no free parameters.

The peak value of the Brillouin gain coefficient is

$$g_0 = \frac{2\pi\,\gamma^2}{nc\rho_0\upsilon\,\lambda_{\mathrm{L}}^2\Delta\nu_{\mathrm{B}}M} \tag{9}$$

which equals 6.4×10^{-12} m/W for the parameters given above. This value is a factor of 2 to 4 times smaller than what is typically measured for fibers [14], possibly because of inhomogeneous broadening of the Brillouin peak. According to (9), it is only the *product* $g_0\Delta\nu_{\mathrm{B}}$ that should be the same

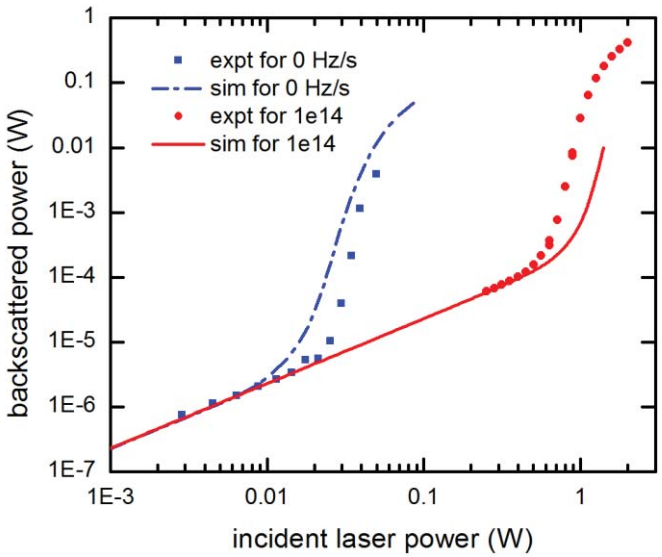

Fig. 2. Comparison of the simulated and experimental [7] total backscattered power for the unchirped and chirped laser sources.

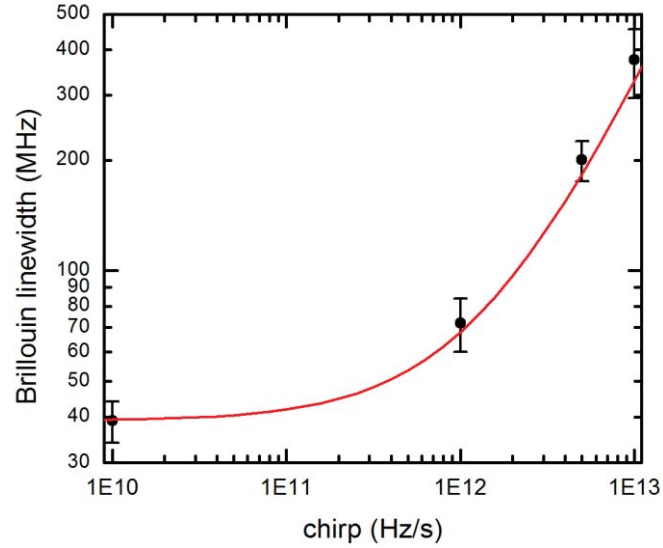

Fig. 3. FWHM $\Delta\nu$ of the Brillouin line as a function of β.

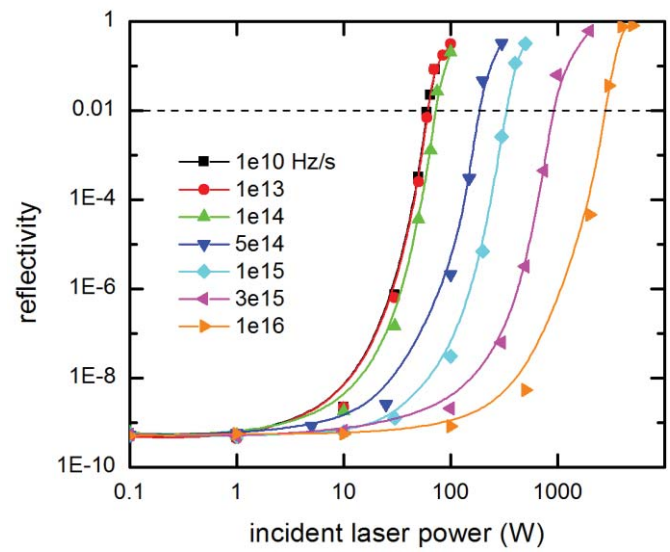

Fig. 4. Brillouin reflectivity for a laser beam with a linear chirp β ranging between 10^{10} and 10^{16} Hz/s that is incident on a short fiber.

for all polarization-scrambling silica fibers pumped at 1.55 μm and not their *individual* two values.

The power spectral density (in dBm/Hz) of the reflected Stokes electric field $E_S(0,t)$ was plotted for each simulation run as a function of frequency up to the Nyquist limit. Lineshape functions were then fit to these spectra. The resulting FWHM are plotted as the dots in Fig. 3 for the long fiber at $P_0 = 1$ mW, well below threshold, for four different chirps. At the two lower chirps β of 10^{10} and 10^{12} Hz/s the lineshapes were found to be Lorentzian, whereas at the two higher chirps of 5×10^{12} and 10^{13} Hz/s the lineshapes were Gaussian. The continuous curve is a plot of the broadening expected from a simple model, namely

$$\Delta\nu = \Delta\nu_B + nL\beta/c \tag{10}$$

which fits the simulation results to within the error bars on the widths. Replacing $\Delta\nu_B$ by $\Delta\nu$ in (9), this increase in the Brillouin bandwidth implies a reduction in the peak gain and hence a higher threshold P_{th} compared to the unchirped case.

IV. Dynamic Results for a Short Passive Fiber Compared to Other Models

Consider a passive delivery fiber having a length of $L = 17.5$ m, a core radius of $r = 13.75$ μm, and a spontaneous Brillouin FWHM of $\Delta\nu_B = 20$ MHz conservatively chosen to be on the low end of the range of linewidths measured for silica fibers [15] so that the peak Brillouin gain is as large as it might be (namely $g_0 = 1.2 \times 10^{-11}$ m/W). All other parameters are taken to be the same as those listed in Secs II and III. The reflectivity is plotted in Fig. 4 for seven different values of the chirp β.

Well below threshold, the reflectivity has a constant value of $R_0 \approx 5 \times 10^{-10}$ independent of chirp and pump power. A heuristic steady-state model [8] for the buildup of the spontaneous Stokes wave from thermal noise predicts that it should be

$$R_0 = \frac{2\pi^2 kT\gamma^2 L_\alpha}{Mn^2\rho_0 v^2 \lambda_L^2 A} \tag{11}$$

where the effective absorption length of the fiber is $L_\alpha \equiv [1-\exp(-\alpha L)]/\alpha$. This model implies $R_0 \approx 3 \times 10^{-9}$ which is only a factor of 6 larger than our simulation value. Similar agreement is found for the long fiber in Sec III: (11) predicts $R_0 \approx 9 \times 10^{-6}$ whereas Fig. 1 has a low-power reflectivity of $R_0 \approx 2 \times 10^{-6}$.

The curves in Fig. 4 cross 1% reflectivity at the threshold incident laser powers, P_{th}. The interpolated crossing points are plotted in Fig. 5 as the squares. At the maximum chirp of 10^{16} Hz/s, the threshold has increased by a factor of 50 compared to an unchirped laser source.

In Fig. 5, the threshold power scales linearly with the chirp β above 10^{14} Hz/s. These results agree with an adiabatic

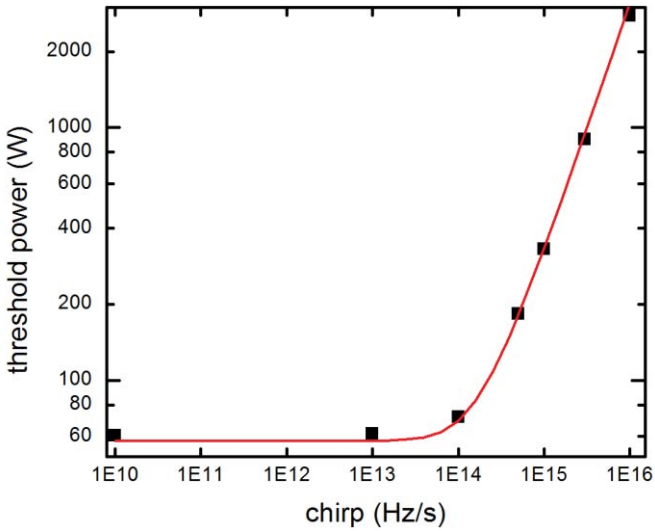

Fig. 5. Threshold power P_{th} as a function of the chirp β. The squares are from the time-dependent simulations and the continuous curve is based on an adiabatic model [7].

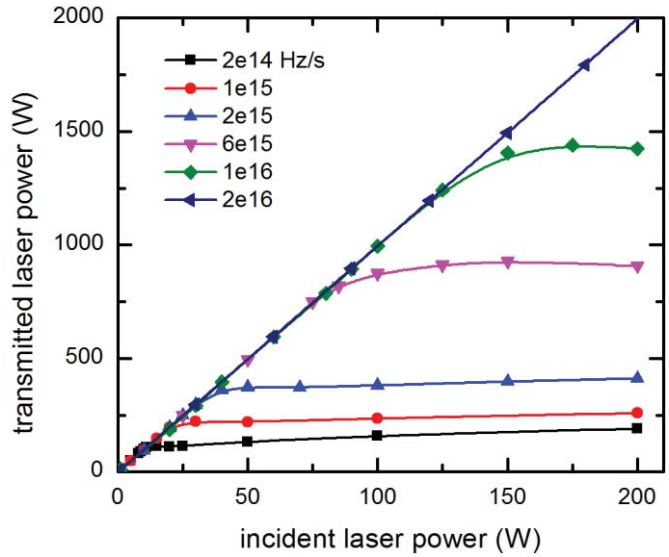

Fig. 6. Transmitted laser power as a function of incident laser power for various chirps.

model, according to which the threshold should increase as $t_{\text{f}}/t_{\text{c}}$ where the fiber transit time is $t_{\text{f}} = nL/c$ and the time required for the pump laser to chirp out of the Stokes bandwidth is $t_{\text{c}} = \Delta\nu_{\text{B}}/2\beta$. Combining a resonant integration [7] of this increase with the familiar [16] factor of 21 for the unchirped threshold value $g_0 P_{\text{th}} L/A$, one obtains

$$P_{\text{th}} = \frac{21A}{g_0 L} \frac{t_{\text{f}}/t_{\text{c}}}{\tan^{-1}(t_{\text{f}}/t_{\text{c}})} \tag{12}$$

plotted as the continuous line in Fig. 5. The agreement with the time-domain simulations is remarkable. Furthermore, one can verify graphically that

$$\frac{t_{\text{f}}/t_{\text{c}}}{\tan^{-1}(t_{\text{f}}/t_{\text{c}})} \approx 1 + \frac{t_{\text{f}}}{2t_{\text{c}}} = \frac{1}{\Delta\nu_{\text{B}}}\left[\Delta\nu_{\text{B}} + \frac{nL\beta}{\text{c}}\right] \tag{13}$$

thereby showing that (10) is also consistent with the adiabatic model.

V. Predicted Output Laser Power for a Short Active Fiber

Chirping enables one to maintain gain in a fiber amplifier by suppressing the power lost to Brillouin backscattering. To demonstrate this effect, we simulated an ytterbium-cladding-doped fiber with length $L = 18$ m and modal radius $r = 13.75$ μm at a laser wavelength of $\lambda_{\text{L}} = 1.064$ μm with a spontaneous Brillouin FWHM of $\Delta\nu_{\text{B}} = 50$ MHz representing a round average of typical linewidths reported in the literature [16]. As a simple, conservative model of 10× amplification, the gain coefficient for both the laser and Stokes-shifted Brillouin waves was set equal to $\zeta = \ln(10)/L$ in (1). (A more accurate model would simultaneously solve the rate equations for the populations of the ground and excited laser levels to compute the gain from a separate pump source [17].) In Fig. 6, values of P_{L} calculated from (8) are plotted versus P_0 for chirps β between 2×10^{14} and 2×10^{16} Hz/s. At low chirps, the transmitted power rolls off when it surpasses threshold. For example, at a chirp of 2×10^{14} Hz/s and incident laser power of 100 W, which is well beyond threshold, in the absence of gain the laser power drops to and levels off at 87 W within the first few meters of the fiber, while the Stokes power correspondingly rises from 0 to 13 W over the same distance. In contrast, with the 10× gain switched on, the laser power drops to a minimum after about 1 m of transit but is then amplified over the remainder of the fiber's length to 215 W, as plotted in Fig. 6; meanwhile the Stokes beam begins to grow a few meters from the rear end of the fiber and attains about 400 W at the front face. At the highest chirp, in contrast, 10× amplification is maintained for incident powers up to 200 W in Fig. 6, resulting in kilowatt output laser powers.

VI. Conclusion

Time-dependent numerical simulations show that SBS in optical fibers can be suppressed by linearly chirping the laser frequency. One significant advantage of this method compared to competing techniques that broaden the incident laser beam with white noise is that a narrow instantaneous linewidth is maintained, enabling coherent combination of the outputs of several fiber lasers for power scaling. Linear chirping allows a mismatch in the length of one amplifier relative to another to be compensated by acousto-optically shifting the frequencies at the input [18].

These dynamic simulations are in good agreement with experimental results for a 6-km fiber. The simulations should therefore also be valid for a short 17.5-m fiber having characteristics appropriate to high-power laser systems. The time-dependent numerical results for a short passive fiber are in good agreement with an analytic adiabatic model, thereby validating use of that model to predict the performance of chirped fiber lasers without requiring the demanding computer overhead of the full time-dependent calculations. The results for a short active fiber indicate that laboratory attainable

chirps enable amplification to kilowatt output powers while maintaining a narrow instantaneous laser linewidth.

ACKNOWLEDGMENT

The authors would like to thank C. R. Menyuk for discussions of numerical methods. Computer programs provided to us by S. M. Wandzura, A. David, M. Horowitz, and R. B. Jenkins guided the writing of our codes, which ran on High Performance Computing Clusters at ARL, Aberdeen, MD, and at USNA Physics Department, Annapolis, MD, with the assistance of R. Witt.

REFERENCES

[1] K. Shiraki, M. Ohashi, and M. Tateda, "Suppression of stimulated Brillouin scattering in a fibre by changing the core radius," *Electron. Lett.*, vol. 31, no. 8, pp. 668–669, Apr. 1995.

[2] A. Kobyakov, S. Kumar, D. Q. Chowdhury, A. B. Ruffin, M. Sauer, S. R. Bickham, and R. Mishra, "Design concept for optical fibers with enhanced SBS threshold," *Opt. Exp.*, vol. 13, no. 14, pp. 5338–5346, Jul. 2005.

[3] V. I. Kovalev and R. G. Harrison, "Suppression of stimulated Brillouin scattering in high-power single-frequency fiber amplifiers," *Opt. Lett.*, vol. 31, no. 2, pp. 161–163, Jan. 2006.

[4] J. B. Coles, B. P.-P. Kuo, N. Alic, S. Moro, C.-S. Bres, J. M. C. Boggio, P. A. Andrekson, M. Karlsson, and S. Radic, "Bandwidth-efficient phase modulation techniques for stimulated Brillouin scattering suppression in fiber optic parametric amplifiers," *Opt. Exp.*, vol. 18, no. 18, pp. 18138–18150, Aug. 2010.

[5] C. Zeringue, I. Dajani, S. Naderi, G. T. Moore, and C. Robin, "A theoretical study of transient stimulated Brillouin scattering in optical fibers seeded with phase-modulated light," *Opt. Exp.*, vol. 20, no. 19, pp. 21196–21213, 2012.

[6] N. Satyan, A. Vasilyev, G. Rakuljic, V. Levya, and A. Yariv, "Precise control of broadband frequency chirps using optoelectronic feedback," *Opt. Exp.*, vol. 17, no. 18, pp. 15991–15999, Aug. 2009.

[7] J. O. White, A. Vasilyev, J. P. Cahill, N. Satyan, O. Okusaga, G. Rakuljic, C. E. Mungan, and A. Yariv, "Suppression of stimulated Brillouin scattering in optical fibers using a linearly chirped diode laser," *Opt. Exp.*, vol. 20, no. 14, pp. 15872–15881, Jul. 2012.

[8] R. B. Jenkins, R. M. Sova, and R. I. Joseph, "Steady-state noise analysis of spontaneous and stimulated Brillouin scattering in optical fibers," *J. Lightw. Technol.* vol. 25, no. 3, pp. 763–770, Mar. 2007.

[9] A. Melloni, M. Frasca, A. Garavaglia, A. Tonini, and M. Martinelli, "Direct measurement of electrostriction in optical fibers," *Opt. Lett.*, vol. 23, no. 9, pp. 691–693, May 1998.

[10] M. O. van Deventer and A. J. Boot, "Polarization properties of stimulated Brillouin scattering in single-mode fibers," *J. Lightw. Technol.*, vol. 12, no. 4, pp. 585–590, Apr. 1994.

[11] R. W. Boyd, K. Rzazewski, and P. Narum, "Noise initiation of stimulated Brillouin scattering," *Phys. Rev. A*, vol. 42, no. 9, pp. 5514–5521, Nov. 1990.

[12] A. David and M. Horowitz, "Low-frequency transmitted intensity noise induced by stimulated Brillouin scattering in optical fibers," *Opt. Exp.*, vol. 19, no. 12, pp. 11792–11803, Jun. 2011.

[13] I. Bar-Joseph, A. A. Friesem, E. Lichtman, and R. G. Waarts, "Steady and relaxation oscillations of stimulated Brillouin scattering in single-mode optical fibers," *J. Opt. Soc. Amer. B*, vol. 2, no. 10, pp. 1606–1611, 1985.

[14] V. Lanticq, S. Jiang, R. Gabet, Y. Jaouën, F. Taillade, G. Moreau, and G. P. Agrawal, "Self-referenced and single-ended method to measure Brillouin gain in monomode optical fibers," *Opt. Lett.*, vol. 34, no. 7, pp. 1018–1020, Apr. 2009.

[15] A. Kobyakov, M. Sauer, and D. Chowdhury, "Stimulated Brillouin scattering in optical fibers," *Adv. Opt. Photon.*, vol. 2, no. 1, pp. 1–59, Mar. 2010.

[16] G. P. Agrawal, *Nonlinear Fiber Optics*, 3rd ed. San Diego, CA: Academic, 2001, ch. 9.

[17] M. W. Wright and G. C. Valley, "Yb-doped fiber amplifier for deep-space optical communications," *J. Lightw. Technol.*, vol. 23, no. 3, pp. 1369–1374, Mar. 2005.

[18] N. Satyan, A. Vasilyev, G. Rakuljic, J. O. White, and A. Yariv, "Phase-locking and coherent power combining of broadband linearly chirped optical waves," *Opt. Exp.*, vol. 20, no. 23, pp. 25213–25227, 2012.

Carl E. Mungan received the B.Sc. degree (Hons.) in theoretical physics from Queen's University, Kingston, ON, Canada, in 1986, and the Ph.D. degree in experimental condensed-matter physics from Cornell University, Ithaca, NY, in 1994.

He conducted post-doctoral research on solid-state laser cooling with Los Alamos National Laboratory, Los Alamos, NM, from 1994 to 1996. He was an Assistant Professor with the University of West Florida, Pensacola, from 1996 to 2000. He has been with the U.S. Naval Academy, Annapolis, MD, since 2000, where he is currently an Associate Professor.

Dr. Mungan is a member of the American Physical Society and the American Association of Physics Teachers.

Steven D. Rogers received the B.S. degree in physics from the University of Maryland, Baltimore, in 2010.

He was with the High-Energy Laser Group, U.S. Army Research Laboratory, Adelphi, MD, in 2010 and from 2011 to 2012.

Naresh Satyan (M'09) received the B.Tech. degree in electrical engineering from the Indian Institute of Technology Madras, Chennai, India, in 2005, and the M.S. and Ph.D. degrees in electrical engineering from the California Institute of Technology, Pasadena, in 2007 and 2011, respectively.

He is currently a Post-Doctoral Scholar in applied physics and materials science with the California Institute of Technology. His current research interests include semiconductor lasers, optical phase and frequency control, coherent optics and optoelectronics, 3-D imaging, and biomedical optics.

Dr. Satyan is a member of the Optical Society of America.

Jeffrey O. White (M'08) received the B.Sc. degree in physics (Hons.) from Brown University, Providence, RI, in 1977, and the Ph.D. degree in applied physics from the California Institute of Technology, Pasadena, in 1984.

He was a Technical Staff Member with the Hughes Research Laboratories, Malibu, CA, a Guest Researcher with the Laboratoire d'Optique Appliquée, Palaiseau, France, and a Humboldt Fellow with the Max-Planck-Institute for Solid State Physics, Stuttgart, Germany. From 1994 to 1996, he was a Professor of physics with Université de Bourgogne, Dijon, France, and from 1996 to 2004, he was the Director of the Laser and Spectroscopy Facility, Materials Research Laboratory, University of Illinois at Urbana-Champaign, Urbana. Since 2005, he has been with the Army Research Laboratory, Adelphi, MD.

Dr. White is a fellow of the Optical Society of America.